Avestia Publishing
International Journal of Civil Infrastructure (IJCI)
Volume: 5, Year 2022
Journal ISSN: 2563-8084
DOI: 10.11159/ijci.2022.014

Effect of Corrosion Location and Transverse Reinforcement on Flexural-Ductile Response of Reinforced Concrete Beams

Safdar Naveed Amini [1], Aditya Singh Rajput [2]
[1,2] Department of Civil Engineering, Indian Institute of Technology Ropar, Rupnagar, 140001 Punjab, India
First. 2018cez0001@iitrpr.ac.in; Second. aditya.rajput@iitrpr.ac.in

Abstract – Concern about premature ageing and deterioration of reinforced concrete (RC) structures primarily stems from reinforcement corrosion. The reinforcement corrosion not only reduces the effective cross-section of reinforcing bars but also causes a severe reduction in the structural performance and service life of RC structures. This study aims to analyze the effect of varying corrosion levels on the load-bearing ability of RC beams configured with varying amounts of transverse reinforcement. The idea pertinent to this study is to develop and validate a 3D finite element numerical model of RC beams and subsequently simulate the corrosion deterioration to assess the effect of corrosion deterioration on the flexural response of RC beams. The beam models have been analyzed with a four-point simply supported bending flexural test. For concrete-steel interaction simulation, the cohesive surface interaction method proved to be most suitable as the results aligned well with the analytical results. Loss of bond in concrete-rebar interface due to decrease in mechanical interlock is calculated. The concrete Damage Plasticity model is adopted for calculating concrete's confined and unconfined strength in tension and compression. A parametric study is also performed to investigate varying corrosion percentages on residual capacity, stiffness, energy dissipation and behaviour of corroded beams. Flexural strength response due to spacing of transverse reinforcements as per different Indian standard codes is analyzed. Spalling stress is calculated analytically and used in simulation data for more precise results. The results indicate a notable reduction in load-deflection behaviour due to concrete spalling, deterioration of rebars ribs, loss in mechanical interlock mechanism and yield strength. The structure undergoes an absolute brittle failure at very high corrosion levels due to a complete steel-concrete bond loss. A good correlation between the developed FE model and experimental load-deflection curves was observed, with variability in ultimate load-bearing capacities of less than 5% for all the cases.

Keywords: Bond slip, Finite element, Mechanical interlock, Rebars corrosion, Reinforced concrete.

1. Introduction

Reinforced concrete structures in marine and humid areas are prone to corrosive chloride media. It results in early deterioration of reinforcing bars due to corrosion. Corrosion of Reinforced Concrete (RC) bars is the most severe problem among the durability issues. World Corrosion Organization (WCO) states that corrosion costs over 3% of the world's Gross Domestic Product (GDP) every year. The main consequences of steel corrosion include a decrease in yield strength, reduction in rebar cross-sectional area and generation of circumferential outward expansive pressure, causing cracking and spalling of concrete cover [1]. Various factors influence corrosion, such as loss of alkalinity due to carbonation and chlorides, insufficient concrete cover, moisture pathways and construction variability in the mix design. These problems will ultimately affect the integrity and load-carrying capacity of the structure [2-3]. Thus, immediate attention is required towards analyzing and quantifying this deterioration cause and loss of structural strength, thereby devising suitable ways for its prevention. The duration of initiation period is analyzed by how swiftly the concrete cover is cracked or spalled. As a result, activating substances such as chlorides and CO_2 penetrate the steel, speeding up the

Date Received: 2022-09-29
Date Accepted: 2022-10-10
Date Published: 2022-11-15

corrosion process [4-5]. The literature study follows stepwise evaluation by various researchers who are discussed next,

a) Mechanical Experiments on Corroded Reinforcement Bars: Almusallam [6] explained a reduction in tensile strength with increased corrosion resulting in brittle failure. Bossio et al. [7] experimentally studied a decrease in rebar elasticity due to an increase in the degree of corrosion. They concluded a reduction in yield strength and elastic modulus with increasing corrosion levels. A similar kind of work has been explained by comparing the effects of uniform and pitting corrosion on structural stability. It is concluded that pitting corrosion is more hazardous than uniform corrosion by making the structure brittle [8].

b) Bond between Concrete and Reinforcement Steel Bars: Almusallam et al. [9] explained variation in bond stress at concrete-rebar interface due to expansive stress development. Amleh and Ghosh [10] modelled the effect of corrosion on bond strength and concluded a sharp decrease in concrete-steel bond strength with increasing corrosion levels. Furthermore, Ogura et al. [11] discovered a reduction in pressure and friction, i.e., bond splitting failure between a steel-rebar interface with varying corrosion levels.

c) Experimental works on Corroded Beams: Lachemi et al. [12] experimented on RC beams with various levels of corrosion and analyzed reduction in load-bearing capacity and increase in displacement with increasing corrosion. Bhargava and Ghosh [13] examined that lateral load-carrying capacity, strength and stiffness reduce with increasing corrosion. Moreover, Rajput and Sharma [14-15] analyzed that inadequate confinement reinforcement in corroded structures significantly reduces ductility, strength and energy absorption. Increased crack widths and deflections deteriorate performance at service loads.

d) Modelling of Corroded Beams: Maaddawy et al. [16] explained an analytical model under maximum slip at the maximum stress for calculating bond stiffness and spalling stresses due to increased corrosion. [17-18] formulated an analytical model for calculating the variation of a cross-sectional area, increased crack spacing and width for pitting and uniform corrosion as explained in Figure.1. Furthermore, Kalias and Rafiq [19] analyzed a finite element (FE) way for corroded structures and formulated a bond deterioration model and local stress-slip law for determining stresses and strains acting on RC beams subjected to flexure.

Various researchers have done a lot of research efforts in the past years to experimentally analyze corrosion-induced damages in rebars. However, none of the studies presented a finite element analysis approach to model the corrosion in rebars embedded in concrete. Since the experimental research is time-consuming, the purpose of this study includes analytical calculations of various reduced properties of steel and concrete and applying them to FE model to validate the experimental data taken from the literature. In this study, a corroded concrete-rebar interface was modelled separately along with spalling stresses and then applied in the FE model for precise results. Finally, a parametric study was also performed to analyze the behavioural response, structural integrity and capacity of the modelled corroded beams under different corrosion scenarios.

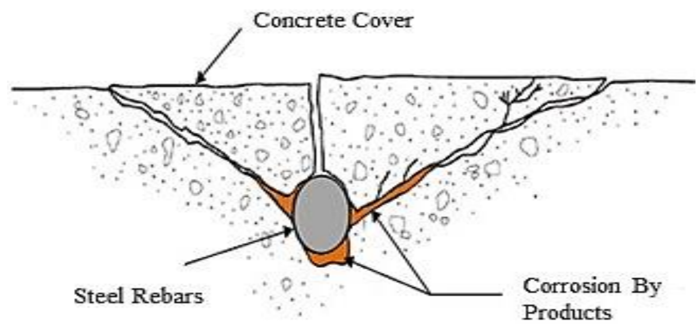

Figure.1 Corrosion cracking and concrete spalling

2. Research Methodology

2.1. Finite Element Modelling

The main objective of the present research work was to develop a comprehensive 3D FE model for corroded and uncorroded RC beams. A non-linear FE model was developed to predict the behavioural response of both types of structures i.e. (corroded and un-corroded) under flexure using ABAQUS 6.14.1. Due to high non-linearity in the FE model, a Dynamic Explicit analysis was opted for simulation as it overcomes the quasi-static complex contact and convergence problems [20]. Three-dimensional 8-noded linear brick reduced integrated elements (C3D8R) were used for describing longitudinal reinforcements, steel plates and concrete. A 2-noded linear 3D truss element (T3D2) was adopted for the stirrups. Steel plates were used to apply loads on the

Beam. Boundary conditions, i.e., fixed and roller supports, were applied to calculate deflections and reaction forces. Concrete and corroded steel were connected using the master-slave interactions. A concrete-rebar slip phenomenon was explained using normal and shear stiffness of structure.

2.2. Concrete Behaviour Model

The concrete Damage plasticity (CDP) model was more suitable for modelling the concrete behaviour when structures show failures and softening behaviour. Inelastic strain, cracking strain and damage related to tension and compression members were calculated analytically along with the softening behaviour. The five different damage parameters used for explaining damage in concrete are explained in Table 1 [20]. This model was developed by Lubliner et al. [21] and was extended by Lee and Fenves [22].

Table 1. Parameters for the CDP model

Symbol	Quantity	Value
ψ	Dilatation angle	37
ε	Flow potential eccentricity	0.1
Fb_0/fc_0	Initial biaxial compressive stress to initial compressive stress	1.16
K_c	Ratio of second stress invariant on the tensile meridian	0.67
λ	viscosity parameter	0.001

2.3. Concrete Zones

Reinforced concrete is divided into three zones, i.e., confined, unconfined and core concrete [23], Fig. 2(a), (b). The confined zone of specimen exhibits more strength than the unconfined zone as it is encountered by forming a cage-like structure due to reinforcements. It is admissible that the inclusion of transverse reinforcements improves structural integrity and resilience. It safeguards the structure, especially under earthquake forces and lateral loads. Stirrups resist shear forces and prevent buckling of longitudinal bars thus improving the structure's ductility [24].

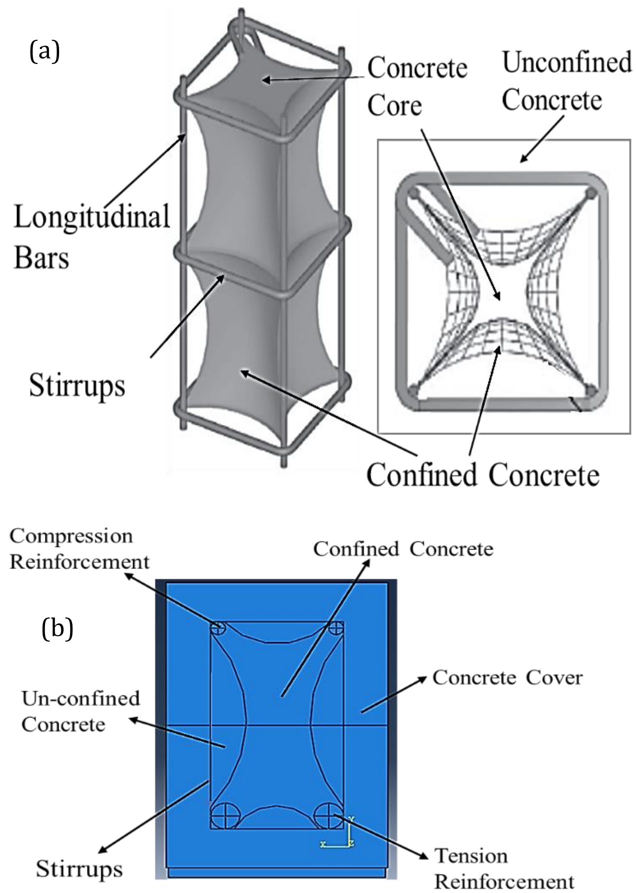

Figure. 2 (a) Different Concrete Zones in a rectangular Beam [23] (b) Reinforced concrete zoning of modelled FE beam

2.4. Confined Concrete Strength

Concrete behaviour under tension is assumed to be linear by resisting tensile stresses caused by bending forces due to applied loads until concrete cracking initiates at the concrete's modulus of rupture [25]. CDP values, damage parameter, inelastic confinement effectiveness coefficient (k_e), lateral adequate confining pressure (f_l') and cracking strains (ε_{cc}) are calculated using the equations [1-4] in a stress-strain model for confined Concrete [26].

$$f_{cc}' = \left(-1.254 + 2.254\sqrt{1 + 7.94\frac{f_l'}{f_c'}} - 2\frac{f_l'}{f_c'} \right) \quad (1)$$

$$\varepsilon_{cc} = \epsilon_{co}\left[1+5\frac{f_{cc}'}{f_c'} -1\right] \quad (2)$$

$$k_e = \frac{\left(1-\frac{s'}{2d_s}\right)}{1-p_{cc}} \quad (3)$$

$$f_l' = 0.5\times k_e \times \rho_s \times f_{yh} \tag{4}$$

2.5. Bond Stress and Slip Calculation

Concrete-rebar bond stress was calculated for beams with different percentages of corrosion levels [19] using the equations [5-8]. The first part of equation 5 explains concrete's influence, and the latter is used for stirrups. The bond loss reduction factor (R) was calculated to investigate the number of corrosion levels in the specimens as per the duration of the current. A reasonable, valid result is expected since many parameters are included in bond stress τ_{max} and rebar-slip (S_1) calculation.

$$\tau_{max} = R\,(0.55+ 0.24\,\frac{C_c}{d_b})\,\sqrt{f_c} + 0.191\frac{A_{tf_{yt}}}{S_s\, d_b} \tag{5}$$

$$R = [A_1+ A_2X] \tag{6}$$

$$S_1 = S_{max} = 0.15\,C_o\,\frac{10}{3}\ln(\frac{\tau_{max}}{\tau 1})+ S_o \ln\,(\frac{\tau 1}{\tau_{max}}) \tag{7}$$

$$\tau_1 = 2.57\,\sqrt{f_c} \tag{8}$$

2.6. Degraded Properties of Concrete and Steel

Circumferential expansive pressure due to corrosion by-products reduces the concrete strength in the cover region. Reduced concrete strength in compression and tensile regions were estimated by Equations [9-13]. Some factors such as number of bars (n_{bar}) and width of cracks (w_{cr}) occurred due to rebar corrosion playing an essential role in calculating the degradation of concrete. Since chlorides and CO_2 ingress reduces the cross-sectional area of rebars, the residual yield strength (f_{yc}) and reduced modulus of elasticity (E_{sc}) of rebars are calculated as follows [27].

$$f_{cc} = \frac{f_c}{1+k\frac{\varepsilon 1}{\varepsilon c}} \tag{9}$$

$$f_{tt} = \frac{f_{cc}}{f_c}\times f_t \tag{10}$$

$$\epsilon_1 = \frac{n_{bar} w_{cr}}{b_o} \tag{11}$$

$$f_{yc} = (1\text{-}0.011X_p)f_y \tag{12}$$

$$E_{sc} = (1\text{-}0.007X_p)E_s \tag{13}$$

2.7. Spalling Stresses Calculation

Increased rebar corrosion results in an enlarged circumferential net outward pressure due to corrosion by-products [28]. Since concrete cover is in an unconfined zone, due to volumetric expansion of rebars, corrosion is in the form of rust, and there is an increase in uniform radial outward pressure (P_{cor}) around the cover zone. This resulted in spalling of concrete cover, calculated by equations [14-16].

$$P_{cor} = \frac{m\,E_{ef}\,D}{90.9\,(1+\vartheta+\psi)\,(D+2\delta 0)} - \frac{2\delta 0\,E_{ef}}{(1+\vartheta+\psi)\,(D+2\delta 0)} \tag{14}$$

$$\psi = \frac{(D+2\delta 0)2}{2C\,[C+(D+2\delta 0)]} \tag{15}$$

$$E_{ef} = \frac{E}{1+\theta} \tag{16}$$

3. Experimental Data considered for FE Models Validation

The experimental data related to a rectangular beam's flexural and shear behaviour was obtained by load-deflection graphs [12]. These beams were considered for the validation of corroded and non-corroded FE-modelled beams. Four levels of reinforcement corrosion, i.e., 5%, 10%, 15% and 20% were subjected in beams for the uniform mass losses in rebars and stirrups. Calculated residual strength of concrete and corroded steel rebars on beams (BM 1-7) with varying corrosion % is explained in Table 2.

The moment of resistance of this Beam is calculated analytically. It is analyzed that the moment of resistance of Beam is greater than its limiting moment of resistance, i.e., ($Mu > Mu_{lim}$). Due to the depth restrictions in the structure, a compression reinforcement was also provided in beams by calculating its factored shear load and shear resistance capacity.

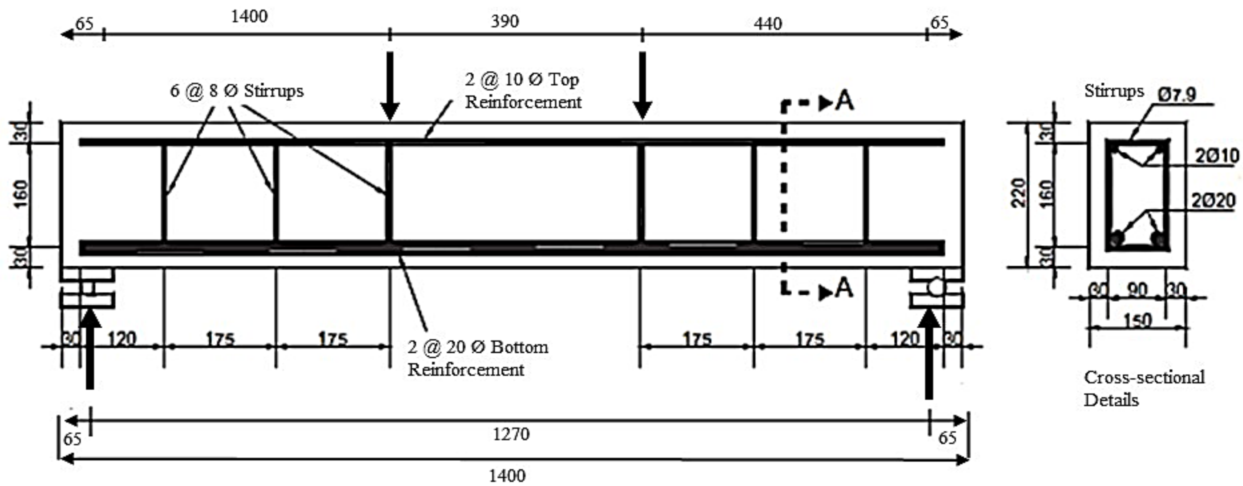

Fig.3 Reinforcement details of Beam Specimen [12]

Table 2: Calculated concrete and steel residual strength of corroded rebars (MPa)

Beam Type	Corrosion Degree (%)	Steel Yield Strength	Stirrups Yield Strength	Reduced Elasticity of Steel	Reduced Elasticity of Concrete	Concrete cover strength	Bottom rebars Bond Stress	Bottom rebars Spalling stress	Top rebars Bond stress	Top rebars Spalling stress
BM-0	0	550	400	200000	26100	31	23	0	21	0
BM-1	5	520	380	193000	22800	23.5	21.11	0.36	19.53	0.38
BM-2	10	490	356	186900	19300	19	19.76	0.72	18.2	0.77
BM-3	15	460	334	179000	12950	12.2	18.44	1.12	17.2	1.22
BM-4	20	425	310	172000	6080	6.32	16.81	1.45	15.67	1.55
BM-5	30	360	265	158000	3320	3.44	14.13	2.17	13.24	2.30
BM-6	40	308	224	144000	1550	1.63	11.32	2.90	10.7	3.10
BM-7	50	240	180	130000	831	0.87	8.5	3.60	8.2	3.80

3.1. Surface-Based Cohesive Modelling

The 3D-FE non-corroded RC beams were modelled using a perfect bond method with steel and concrete elements as an embedded system under interactions. Using uniform bonding, their interface nodes were connected with tie constraints for rebar-concrete bonds. A concrete-rebar slip phenomenon was modelled for modelling corroded beams using a surface-based cohesive behaviour approach. It was analyzed by calculating the actual-bond slip relationship between steel and concrete using traction separation law [29].

The normal (K_{nn}) and shear stiffness (K_{ss}, K_{tt}) values were calculated and applied under the cohesive traction separation section by eq. [17-18].

$$K_{ss} = K_{tt} = \frac{\tau_{max}}{S_1} \quad (17)$$

$$K_{nn} = 100K_{tt} \quad (18)$$

4. Results and Discussions

This work aimed to compare and quantify the load-deflection (L-D) curves obtained from experimental data and FE modelling. A beam model with no corrosion was

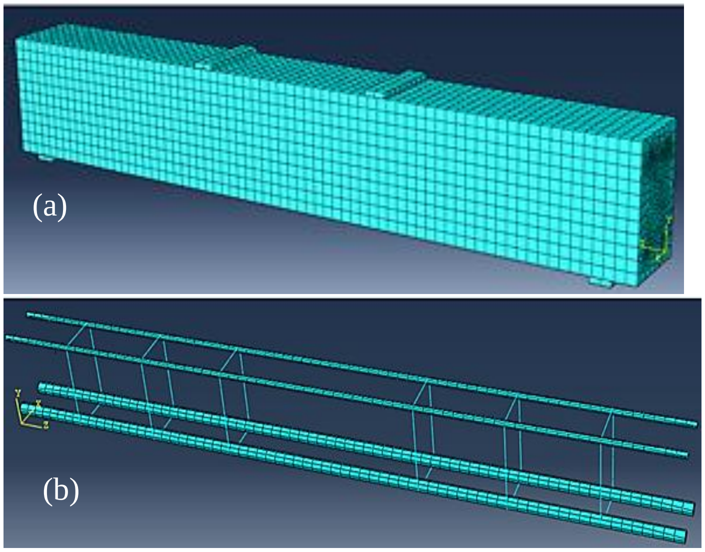

Fig.4(a) 3D FE RC Beam (b) Reinforcement explanation

modelled using a perfect bond case. Different beams for corrosion were modelled to analyze the four levels of corrosion percentages i.e., 5, 10, 15, and 20. The modelled beams along with their reinforcement detailing is explained in Figures 4 (a), (b). Simulations were performed and the obtained results were discussed in Figures 5 (a) to 5 (e). The following graphs explain the mid-span load-displacement reactions of beams with varying corrosion percentages. The experimental results were compared with the simulation (SIM) results. It is evident that increasing corrosion is inversely proportional to the stiffness and load-bearing capacity of the structure. Moreover, a good matching between finite element and experimental load-deflection curves is observed with variability in ultimate load-bearing capacities of less than 5% for all cases.

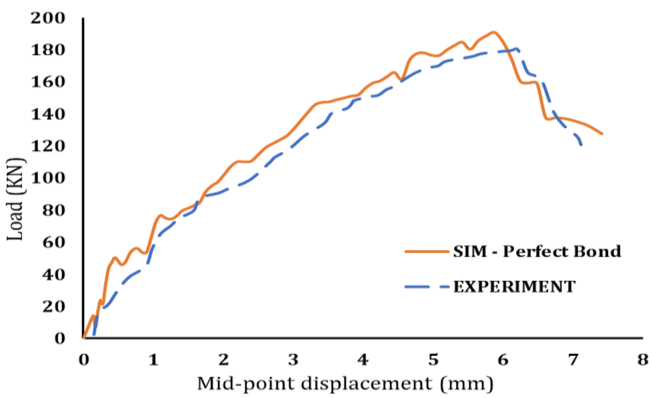

(a) Zero reinforcement loss

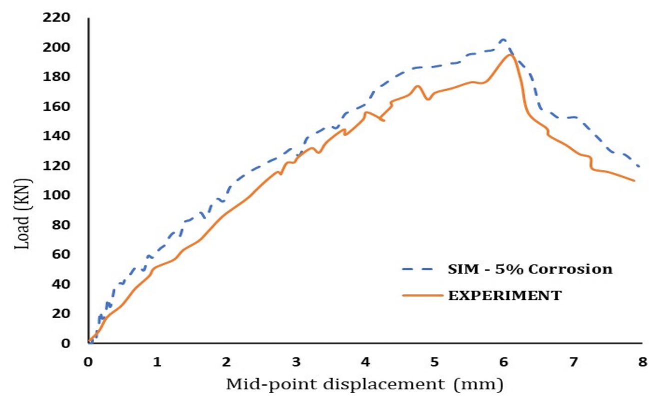

(b) 5% reinforcement loss

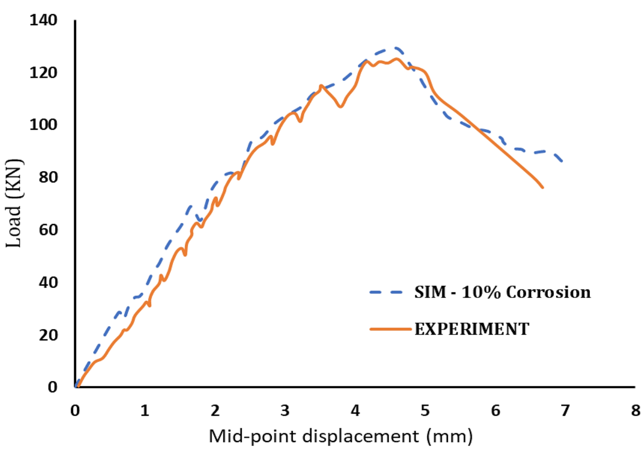

(c) 10% reinforcement loss

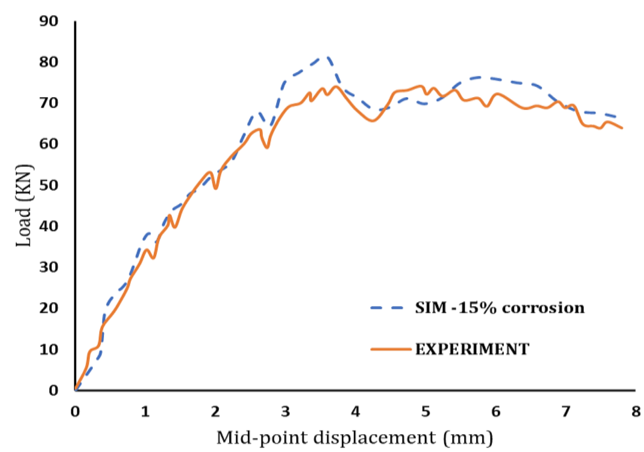

(d) 15% reinforcement loss

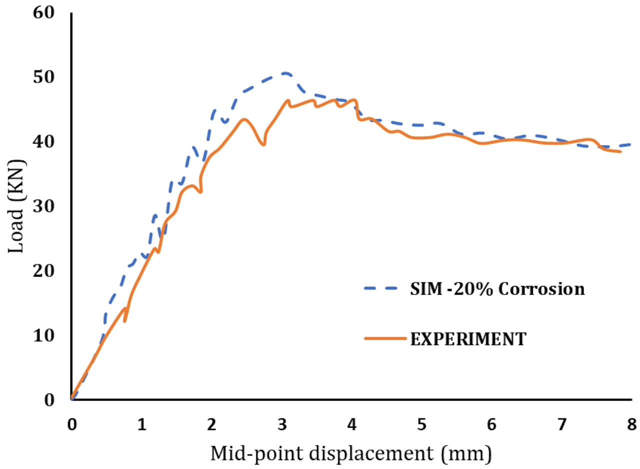

(e) 20% reinforcement loss

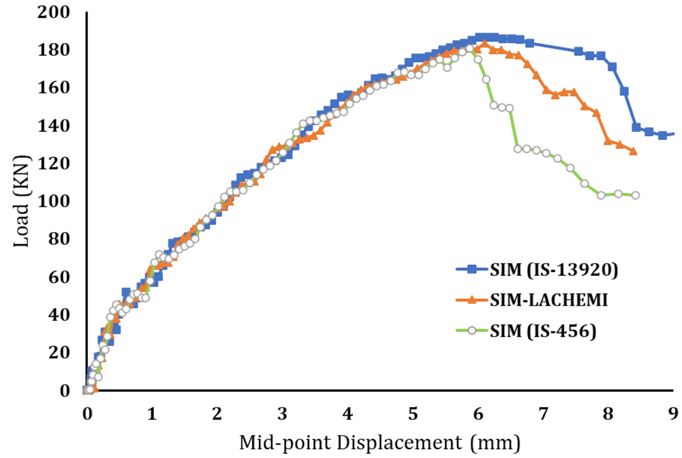

(f) Reinforcement ductility comparison

Fig. 5 Mid-span Load-Displacement curves for Experimental and FE Beams with Varying Corrosion

4.1. Parametric Study

An elaborative study was conducted to further enhance the understanding of corrosion behaviour on different areas of structure. Nineteen 3D FE models were modelled and simulated under static monotonic loading. Seven beams were utilized for the experiment-numerical validation process and the remaining beams were utilized for elaborative parametric study. The dimensions, boundary conditions, and loading were kept the same during all beam models. Calculated steel and concrete material properties were used in beams BM (8-17) along with the corrosion location change as explained in Table 3.

Table 3: Finite element 3d models used in the parametric study

Beam Notation	Cross-section	Description
BM 8-12	Corrosion in Top bars only	Reduced steel and concrete properties- Compression bars.
BM 13-17	Corrosion in Bottom bars only	Reduced steel and concrete properties- Tension bars.
BM 18	Ductile detailing (IS-456)	Spacing of stirrups as per IS-456:2016
BM 19	Ductile detailing (IS-13920)	Ductile reinforcement detailing as per IS 13920:2016

4.1.1. Effect of Corrosion in Compression and Tension Zone

A four-point bending test was performed in this study to understand the flexural strength of structures with various corrosion levels and locations. five FE beams (BM 8-12) were modelled to analyze the effect of corrosion on RC beams only in the compression rebars. As anticipated, compression rebars resulted in a slight reduction in the flexural capacity of Beam as shown in Figure 6(a). It is estimated that this reduction could be due to concrete cover cracks in compressive zone and half the cross-sectional area compared to bottom bars. Similarly, five FE beams (BM 13-17) were modelled to analyze the corrosion effect in tension rebars [30]. It was observed that there is a sharp decrease in flexural strength of corroded beams with an increase in corrosion percentages due to a reduction in the rebar's cross-sectional area, as shown in Figure 6(b). It is also analyzed that after 20% corrosion, the load bearing capacity of the structure reduces to almost one-third and the structure lacks its structural integrity showing a brittle failure.

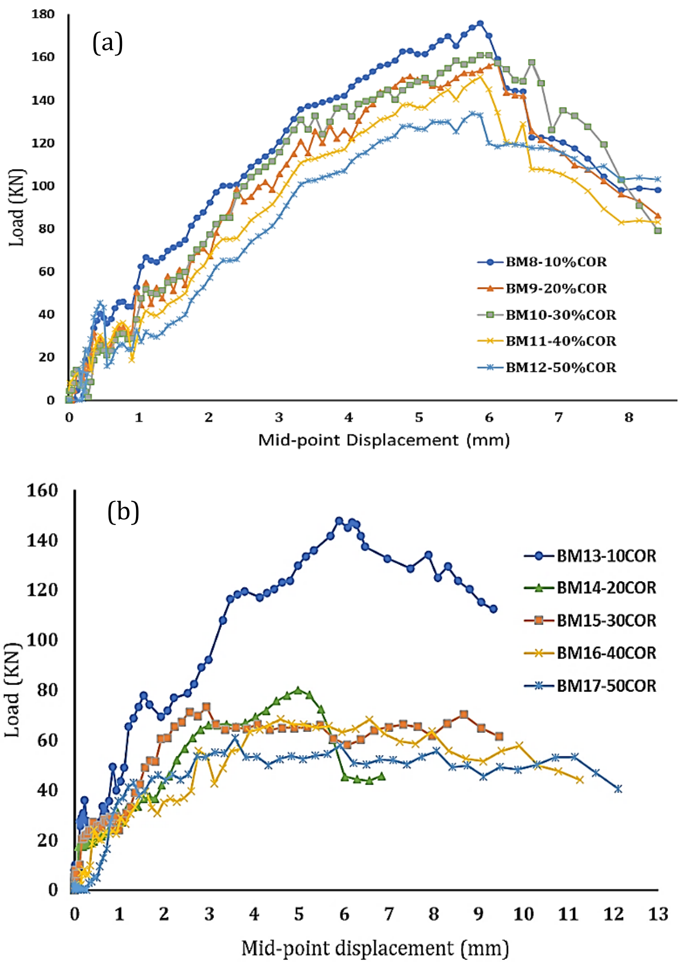

Fig.6 (a) Variation of Corrosion in Compression Zone and (b) Variation of Corrosion in Tension Zone

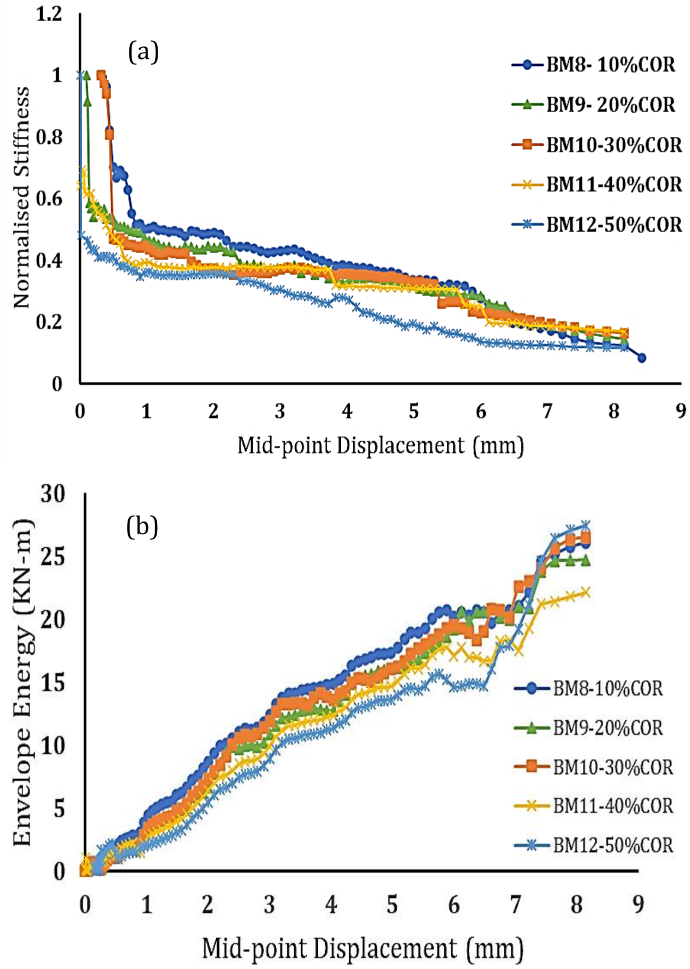

Fig.7 (a) Normalised stiffness curves (b) Energy-dissipation displacement curve

4.1.2. stiffness and energy dissipation degradation in Compression Zone:

For further research, the influence of corrosion on stiffness and energy dissipation of Beam only in the compression zone is evaluated. Calculated normalized stiffness at every displacement level is explained in figure7 (a) and figure 7(b) explains the dissipated energy at mid-point displacement of modelled RC beams. Interestingly, as the corrosion increases from 10% to 50 % i.e., (BM8-12), there is only a slight degradation in the stiffness and dissipation energy of RC beams. It is concluded that the presence of corrosion only in compression longitudinal bars does not impact much the structure's strength, stiffness and energy dissipation.

4.1.3. stiffness and energy dissipation degradation in Tension Zone:

Similar research is done on the influence of corrosion on stiffness and energy dissipation only in the Tension zone of RC columns. Figure 8 (a) explains the normalized stiffness (calculated at every level of displacement level) and figure 8(b) explains the dissipated energy at mid-point displacement. It is evident that the increase in corrosion from 10% to 50% i.e., (BM13-17), results in a rapid decline in stiffness and dissipation energy of RC beams. Due to lack of stiffness at high corrosion levels, structural integrity of Beam reduces and the Beam fails as a brittle failure. It was concluded that the presence of corrosion only in longitudinal tension bars of RC beams plays an important role in structure strength, stiffness and energy dissipation.

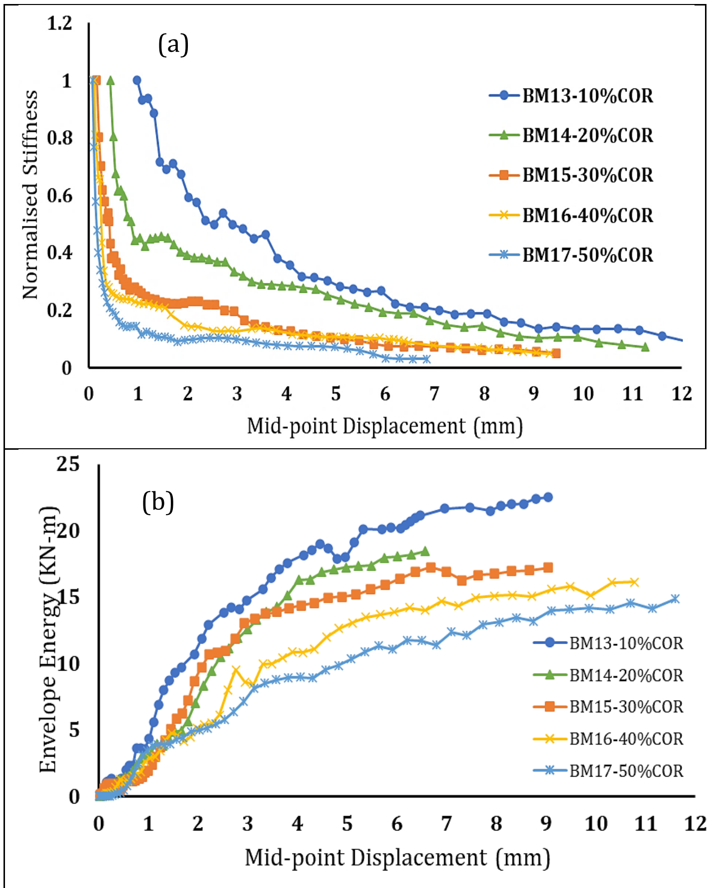

Fig.8 (a) Normalised stiffness curves (b) Energy-dissipation displacement curve

4.1.2. Ductile Detailing of Stirrups

Ductile detailing on modelled RC beams was done by reducing the spacing of stirrups as per Indian standard (IS) codes i.e., IS-13920 and IS-456. This study aimed to understand the structure's ductile response at various Indian seismic zones by varying the stirrups spacings. BM-18 is modelled as per IS-456 [31] and BM-19 as per IS-13920 [32]. Figure 2 (f) compares experimental results with the simulated results obtained using the IS codes. It was interesting to observe that the structure's flexibility improves when reinforcements are designed as per IS codes. It was analyzed that the structure's ductility improves by reducing the stirrups spacings and increasing the number of transverse struts. Thus, the structure behaves more resilient under lateral and earthquake forces.

5. Conclusion

In this work, a comparative assessment was done by modelling a 3D FE simulation for corroded and un-corroded RC beams and comparing their results with the experimental work taken from the literature. A dynamic explicit technique along with the CDP model was used to model beams. The perfect bond method was adopted for non-corroded beam modelling. The cohesive surface technique and master-slave interactions were utilized for corroded beams to connect steel with concrete. Concrete-rebar slip phenomenon was explained and used in a model using normal and shear stiffness between steel and concrete It was analyzed that increasing corrosion is inversely proportional to stiffness and load-bearing capacity of structure. Also, the presence of corrosion only in the compression zone reduces the load-bearing ability of a structure to less extent. Still, the structural strength reduces severely when corrosion is present in the tension zone. Furthermore, the stirrups' spacing as per Indian standard codes increased the structure's ductility, making it resilient under seismic and lateral forces. A good correlation between finite elements and experimental load-deflection curves is observed with variability in ultimate load-bearing capacities of less than 5% for all cases.

Nomenclature			
A_1, A_2	0.861, -0.014: for 1 Amp current	K_{nn}	Stiffness in normal direction
A_t	Total cross-sect. area of stirrup within S_S	K_{ss}, K_{tt}	Stiffness in shear direction
c_C	One-half clear spacing between rebar	m	Corrosion percentage
D	Diameter of steel bar (tension and compression) mm	n_{bar}	Number of bars (in compression and tension zones)
d_b	Diameter of the rebar	R	Bond loss reduction factor, 1 for non-corroded
E_s	Modulus of elasticity of rebar	RC	Reinforced concrete
E_{ef}	Effective elastic modulus, MPa	S'	Centre to centre stirrups spacing

E	Elastic modulus of concrete, MPa	S_S	Spacing of the stirrup
f'_{cc}	compressive strength of confined concrete	S_o	0.15, 0.4 for plain and reinforced concrete.
f_y	Yield strength of rebar, MPa	w_{cr}	Width of crack (cover region crack)
f'_l	Effective lateral confining pressure	ε_{co}	Strain at max. compressive strength
f_{yh}	Yield strength of rebars, MPa	ε_{cc}	Strain values Increase with confined concrete
f_{yt}	Yield stress of the stirrup.	τ_{max}	Bond stress
f_{cc}	Reduced compressive concrete cover strength	ε_c	Strain at maximum compressive strength i.e. (0.002)
f_{tt}	Reduced tensile strength of cover	ε_1	Strain based on corrosion % and crack width
f_c	Concrete compressive strength	δ_0	Thickness of porous zone i.e., 0.001 (mm)
FE	Finite element	θ	Creep coefficient (2.35) (as per CSA standard)
GDP	Gross Domestic Product	ν	Poisson's ratio (0.2)
k	Constant = 0.1 (for ribbed medium diameter bars)	X_p	Corrosion percentage
k_e	Confinement effectiveness coefficient	WCO	World Corrosion Organization

References

[1] A. L. Sakkaf, "Modelling of corroded reinforced concrete beams," Ph.D. dissertation, Dept. Civil Eng., King Fahd Univ., Dhahran, Saudi Arabia.

[2] M. Sompura, M. and N. Kwatra, "Finite element analysis of corroded RC beams," Ph.D. dissertation, Dept. Civil Eng., Thapar Univ., Patiala, India.

[3] H.M. Noh and Noor, N.M., "Structural Effects of Reinforced Concrete Beam Due to Corrosion," in *Proceedings of the E3S Web of Conferences*, Poland, 2018, vol. 34, 01024.

[4] J.M. Wachira, "Effects of chlorides on corrosion of simulated reinforced blended cement mortars," International journal of Corrosion, vol. 13, pp.1-7, 2019.

[5] A.A Abouhussien and A.A. Hassan., "Experimental and empirical time to corrosion of reinforced concrete structures under different curing conditions,". Advances in Civil Engineering, vol. 2014, pp. 1-9, 2019.

[6] A.A. Almusallam, A.S. Gahtani and A.R. Aziz, "Effect of degree of corrosion on the properties of reinforcing steel bars,". Construction Building material, vol. 15, Issue 8, pp. 361-368, 2001.

[7] Bossio.A, Monetta and Belluci. F, "Modelling of concrete cracking due to corrosion process of reinforcement bars,". Cement and Concrete Research, vol. 71, pp. 78-92, 2015.

[8] H.S. Lee and Y.S. Cho, "Evaluation of the mechanical properties of steel reinforcement embedded in concrete specimen as a function of the degree of reinforcement corrosion,". International Journal of Fracture, vol. 157, pp.81-88. 2009.

[9] A.A. Almusallam, A.S. Gahtani and A.R. Aziz, "Effect of reinforcement corrosion on bond strength,". Construction and Building Material, vol.10, pp.123-129, 1996.

[10] L. Amleh and A.Ghosh, "Modelling the effect of corrosion on bond strength at the steel–concrete interface with finite-element analysis,". Canadian Journal of Civil Engineering, vol. 33(6), pp. 673-682, 2006

[11] N. Ogura, J.E. Bolander and T. Ichinose, "Analysis of bond splitting failure of deformed bars within structural concrete,". Engineering Structures, vol. 30 (2), pp. 428–435, 2008.

[12] M. Lachemi, N.Al. Bayati and M. Sahmaran, "The effect of corrosion on shear behaviour of reinforced self-consolidating concrete beams,". Engineering Structures, vol.79, pp.1-12, 2014.

[13] K. Bhargava, A.K. Ghosh, Y. Mori and S. Ramanujan, "Models for corrosion-induced bond strength degradation in reinforced concrete- Analytical and empirical models," Nuclear Engineering and Design, vol. 237(11), pp.1140-1157, 2007.

[14] A.S. Rajput and U.K. Sharma, "Corroded reinforced concrete columns under simulated seismic loading," Engineering Structures, vol. 171, pp. 453-463, 2018.
[15] A.S. Rajput and U.K. Sharma, "Performance of aged reinforced concrete columns under simulated seismic loading, "Engineering Structures, vol. 20(3), pp. 453-463, 2019.
[16] El. Maaddawy, K. Soudki and T.Cooper, "Analytical model to predict nonlinear flexural behaviour of corroded reinforced concrete beams," ACI Structural Journal, vol.102(4), pp. 550-559, 2005.
[17] D. Coronelli and P. Gambarova, "Structural assessment of corroded reinforced concrete beams: modelling guidelines," Journal of Structural Engineering, vol. 130(8), pp. 1214-1224, 2004.
[18] F. Biondini and M. Vergani, "Deteriorating beam finite element for nonlinear analysis of concrete structures under corrosion,". Structural Infrastructural Engineering, vol. 11(4), pp. 519-532, 2015.
[19] A.N. Kallias and M.I. Rafiq, "Finite element investigation of the structural response of corroded RC beams,". Engineering Structures, vol. 32(9), pp. 2984-2994, 2010.
[20] Abaqus 6.14 Documentation. Providence, RI: Dassault Systems. (Accessed: 25 March 2022)
[21] J. Lubliner, J. Oliver and E. Onate "A plastic-damage model for concrete,". International Journal of Solids Structure, vol. 25(3), pp. 299-326 1989.
[22] J. Lee and G.L. Fenves, "Plastic-damage model for cyclic loading of concrete structures," Journal of Engineering Mechanics., vol. 124(8), pp. 892-900, 1998.
[23] N. Subramanian, "Design of confinement reinforcement for RC columns, "Indian Concrete Journal., vol. 85(6), pp. 19-29, 2011.
[24] D.C. Kent and R. Park, "Flexural members with confined concrete Journal of Structural Engineering, vol. 97(7), pp. 1969-1990, 1971.
[25] B. Mander and R. Park, "Theoretical stress-strain model for confined concrete," Journal of Structural Engineering, vol. 114(8), pp. 1804-1826, 1988.
[26] T. El Maaddawy, K. Soudki and T. Cooper, "Analytical model to predict nonlinear flexural behaviour of corroded reinforced concrete beams,". ACI Structural Journal, vol. 102(4), pp. 550-559, 2005.
[27] P.S. Mangat and M.S. Elgarf, "Flexural strength of concrete beams with corroding reinforcement," Structural Journal, vol. 96(1), pp. 149-158, 1999.
[28] El Maaddawy and K. Soudki, "A model for prediction of time from corrosion initiation to corrosion cracking,". Cement Concrete composition, vol. 29(3), pp.168-175, 2007.
[29] J. Henriques, J.D. Silva, L.S. and Valente, I.B., 2013. Numerical modelling of composite Beam to reinforced concrete wall joints: Part I: Calibration of joint components. Engineering Structure, 52, pp.747-761.
[30] S.M. Allam, M.S. Shoukry, G.E. Rashad and A.S. Hassan, "Evaluation of tension stiffening effect on the crack width calculation of flexural RC members," Alex. Engineering Journal., vol. 52(2), pp. 163-173, 2013.
[31] BIS 456:2016, Plain and reinforced concrete-Code of Practice. Bureau of Indian Standards, New Delhi, India,2016.
[32] BIS 13920:2016, Ductile Detailing of Reinforced Concrete-Code of Practice. Bureau of Indian Standards, New Delhi, India, 2016.